

# Two methods for tracking small animals in SPECT imaging

R. A. Kerekes<sup>a</sup>, J. S. Goddard<sup>a</sup>, S. S. Gleason<sup>a</sup>, M. J. Paulus<sup>a</sup>, A. G. Weisenberger<sup>b</sup>, M. F. Smith<sup>b</sup>, B. Welch<sup>b</sup>

<sup>a</sup>Oak Ridge National Laboratory, Oak Ridge, TN 37831

<sup>b</sup>Thomas Jefferson National Accelerator Facility, Newport News, VA 23606

## ABSTRACT

High-resolution single photon emission computed tomography (SPECT) and X-ray computed tomography (CT) imaging have proven to be useful techniques for non-invasively monitoring mutations and disease progression in small animals. A need to perform *in vivo* studies of non-anesthetized animals has led to the development of a small-animal imaging system that integrates SPECT imaging equipment with a pose-tracking system. The pose of the animal is monitored and recorded during the SPECT scan using either laser-generated surfaces or infrared-reflective markers affixed to the animal. The reflective marker method measures motion by stereoscopically imaging an arrangement of illuminated markers. The laser-based method is proposed as a possible alternative to the reflector method with the advantage that it is a non-contact system. A three-step technique is described for calibrating the surface acquisition system so that quantitative surface measurements can be obtained. The acquired surfaces can then be registered to a reference surface using the iterative closest point (ICP) algorithm to determine the relative pose of the live animal and correct for any movement during the scan. High accuracy measurement results have been obtained from both methods.

**Keywords:** small animal imaging, SPECT imaging, small animal tracking, pose tracking

## 1. INTRODUCTION

Efficient methods for testing new drugs are very important to the pharmaceutical industry. The ability to screen test subjects for effects of a particular drug is an essential element in the process of product development. Small animals are essential for pharmaceutical testing, and mice in particular are useful for modeling human diseases. Efforts to scale down clinical medical imaging systems for smaller subjects have allowed medical researchers to obtain high-resolution computed tomography (CT) images of small animals for disease studies. Noninvasive imaging techniques such as X-ray CT and positron emission tomography (PET) have been developed for small animal medical imaging applications. For example, small animal imaging is used in cancer research to monitor tumor growth and regression in mice.

While anatomical models are useful for studying drug effectiveness, it is very often desirable to screen test subjects for physiological effects of a drug. PET and single photon emission computed tomography (SPECT) are among current techniques used for functional medical imaging. Because test subjects must be kept alive during the screening process in order to monitor functional processes, either the animal must remain motionless for the duration of the scan or its movements must be measured and recorded with a high degree of precision and accuracy. Although sedation and physical restraint can be used to impede animal motion for this type of medical scan, both methods have the potential to alter the neurological and physiological processes that are being studied. By instead using optical methods to track the position of the animal during a scan, the physiology of the animal is kept free from physical and chemical effects that could interfere with the control of the pharmaceutical screening process. The Department of Energy Oak Ridge National Laboratory (ORNL) and Thomas Jefferson National Accelerator Facility (Jefferson Lab), in collaboration with Royal Prince Alfred Hospital in Sydney, Australia, are developing a high-resolution SPECT-based system to image unrestrained, un-anesthetized small laboratory animals.<sup>1</sup> The optical-based animal position tracking apparatus is presently under development at ORNL.<sup>2</sup> Initially, the apparatus will track the position and pose of the animal's head so that a rigid body registration can be assumed. A gantry system allows for the positioning of a tube in which the mouse will be allowed to rest and/or roam. The system concept is shown below in Figure 1.

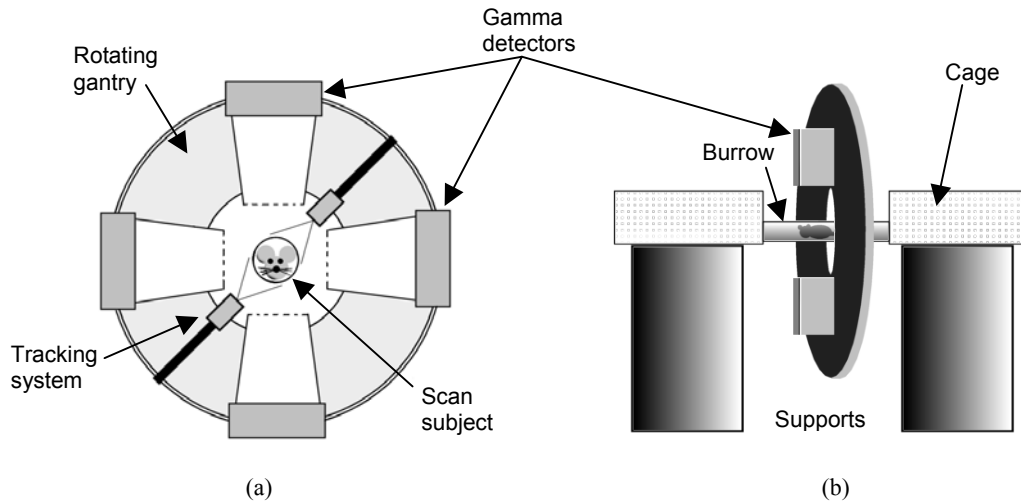


Figure 1. (a) Front view and (b) side view diagrams of system concept.

This paper discusses two different methods for pose tracking that are currently being developed. The first method involves computer-based recognition of infrared (IR) reflective markers attached to the moving subject (Figure 2(a)). In this method, a pair of stereoscopically oriented cameras acquires a synchronized pair of frames so that each pair consists of two views of an arrangement of markers at a certain point in time. For each stereo pair acquired by the cameras, an algorithm is used to locate the reflectors in each of the two images and calculate their position and orientation in three-dimensional space relative to the cameras. If the reflectors are affixed to a rigid body, then the configuration of the reflectors seen by the cameras can be directly translated to the relative pose of the body. The algorithms used to calculate pose in this method are fast enough that pose measurements can be performed in real time at a rate of 5-10 measurements/second while the subject is undergoing a scan, allowing for immediate notification to the user if any tracking problems are encountered during the scan. The pose data is recorded to a file with a global timestamp and can later be merged with time-stamped SPECT scan data to correct for any motion and tomographically reconstruct an accurate depiction of the scanned area.

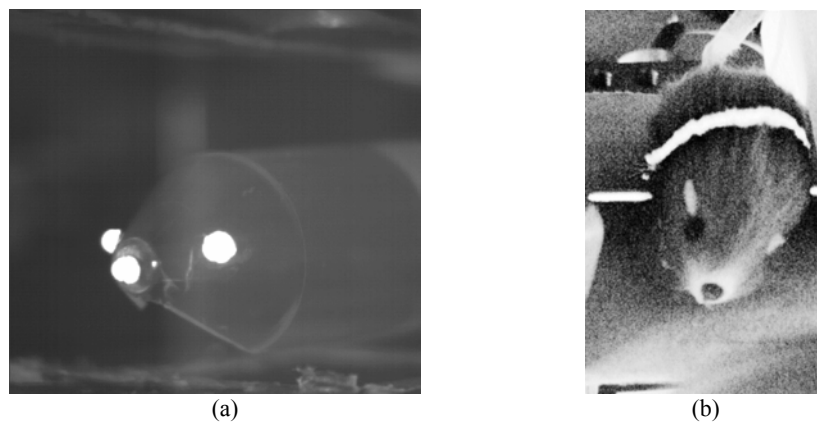


Figure 2. Photographs of (a) reflective markers on plastic tube and (b) laser profiling test subject illuminated by a sheet of light.

The second method for pose tracking uses a laser-based range scanning system to acquire surface data of the moving subject and register them to a reference surface to determine a change in pose. In this method, a laser line is projected onto the surface of the animal, swept back and forth across the animal's body, and viewed at an angle by a camera, thus appearing to the camera as a profile of the subject (Figure 2(b)). The same cameras used in the reflective marker

tracking system are used in the laser tracking system to view a pair of laser lines projected onto either side of the animal. A surface is compiled by forming an array of profiles generated at different positions along the body of the animal. Unfortunately, until the laser profiling system is calibrated, the scale of each dimension of the surface has no practical meaning. By using a three-step technique to calibrate the system, these surfaces can be compared against one another to measure the position of the animal in meaningful units. The iterative closest point (ICP) algorithm<sup>3</sup> is useful for registration of one surface to another surface to determine the transformation between the two. This algorithm is much more computationally intensive than that used in the first method and is unsuitable for real-time pose measurement; however, if surfaces are acquired and stored during the scan, the algorithm can be used off-line to determine pose information and provide motion correction for the corresponding SPECT data.

## **2. TECHNICAL APPROACH**

Pose tracking can be used in conjunction with SPECT image acquisition on live animals in order to correct for animal motion during the scan. Normally changes in position of an animal during a SPECT scan would cause some degree of error in the acquired SPECT data; however, if the position of the animal is known at all times during the scan, the SPECT data can be properly adjusted to compensate for any movement. Two methods for repeatedly calculating the relative position of an animal in a restricted area of movement are discussed in this paper. The laser profiling method is presented as a possible alternative to the reflective marker method, as the former method has certain advantages that could prove to facilitate the live animal scanning process.

### **2.1 Pose tracking using IR reflective markers**

This section describes the general principle of reflective marker pose tracking and the method by which pose parameters are calculated.

#### **2.1.1 General principle**

The reflective marker tracking system measures the animal's head motion through external markers and infrared imaging. Two optical cameras in a stereo configuration are used to measure the 3D point coordinates of the markers located on the animal's head. Infrared (IR) illumination at a wavelength invisible to the animal (850 nm) is used to minimize the impact of the measurement on the animal. To facilitate image segmentation, the markers are retro reflective and require that the illumination be directed coaxially along the camera's optical axis. Figure 3 shows the concept where partially reflecting mirrors are used to direct IR illumination towards the tube. The tube itself is under development and a prototype made of a special glass is presently being fabricated. This material has high transmission to IR at this wavelength but is opaque in the visible range to 700 nm. To use this approach for accurate measurement requires that both intrinsic and extrinsic calibration initially be performed for each camera. Then, the six-degree of freedom coordinate transformation between cameras is calculated. This is an offline operation not required for 3D measurement during SPECT imaging. During normal operation, a minimum of three marker 3D locations is used to calculate full position and orientation (pose) of the head and to track the pose from frame to frame.

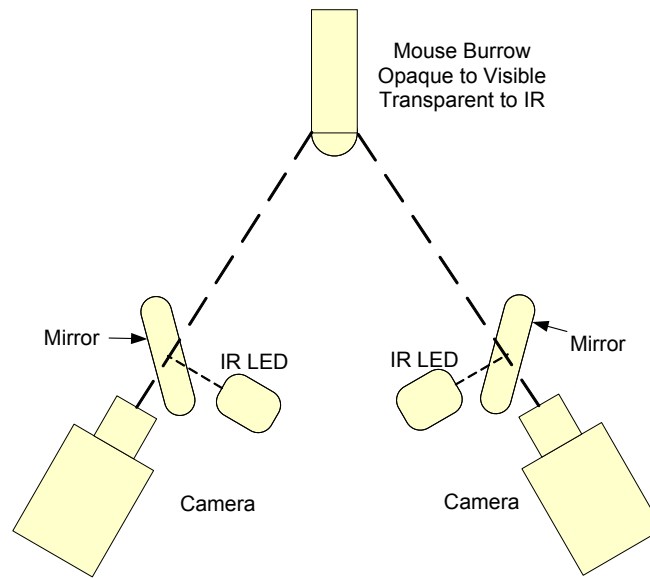


Figure 3. Diagram of tracking system cameras and optics showing arrangement of infrared illumination coaxial with camera optical axis.

### 2.1.2 Calculation of pose parameters

From each acquired image of the retro-reflective markers, the marker regions are segmented via simple thresholding and the centroid of each is calculated. A minimum of three points is required although more are desirable for redundancy and accuracy. The fundamental matrix and the correspondence condition are used to assign matches between the points in each image by finding the minima in each row and column of an  $n$  point match matrix where  $n$  is the number of markers in each image. For each valid point found, the 3D coordinates relative to the second camera are transformed to the frame of the reference camera so that all coordinates are referenced to the same frame. As given in Hartley et. al., the image plane coordinates and camera origin define a 3D line for each camera and marker point.<sup>4</sup> These lines, when extended to the 3D point location, approach each other but are likely to be skewed and do not intersect due to noise and measurement error. The midpoint of the line connecting the closest points of approach for these two 3D lines defines the location of the marker point. The result from this measurement is a set of 3D coordinates relative to the reference camera. While one or more points can define a translation between the reference camera and the head reference frame, three or more are needed to define an orientation plane so that the three rotation parameters can be calculated. A 3D model is defined for this head-centered frame and a best fit of 3D points to the model is used to determine the correct point assignment. Horn's method is used to calculate the transformation and resulting error.<sup>5</sup> The complete pose of the mouse frame with respect to the camera is then calculated.

## 2.2 Pose tracking using laser profiling

This section describes the general principle of laser profile pose tracking and the method used for calibrating the profiling system.

### 2.2.1 General principle

Laser profiling is an alternative method for animal tracking. The laser profiling method uses laser-generated surfaces rather than a set of fixed markers to determine the position of the animal at a certain point in time. A surface is defined as the collection of a number of individual "profiles," each of which is generated by a laser line projected onto and swept across a surface. This sheet of light is dispersed at every point at which it intercepts the surface, causing the surface to appear as if it were wrapped in a thin belt of bright light. If this belt of light were viewed from the same point from which the light emanates, it would appear simply as a straight line; however, when viewed at an angle, the belt of light appears to follow the height contour of the surface along the projection line. Thus, the laser illuminates the surface in such a way as to form a profile of the surface along a particular line. The position of the laser beam projection can then be shifted to reveal surface contours along other lines, and these profiles can be combined to form a two-dimensionally

sampled three-dimensional surface. An example of a pyramid-shaped surface acquired without calibration is shown in Figure 4(a).

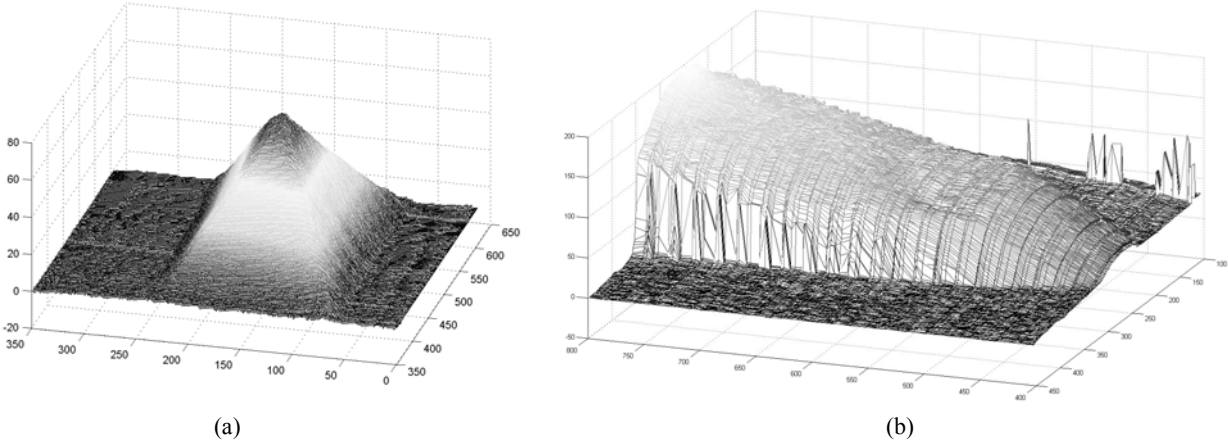


Figure 4. Laser-generated surface samples of (a) 1cm x 1cm base pyramid-shaped structure and (b) a human finger.

Each profile acquired by the camera is comprised of a number of “rangels,” or range pixels. The cameras used in the experimental setup provide functionality for automatically converting individual frames of a laser line into a set of rangels. Height data of the scanned surface is extracted from each profile by measuring the height of each rangel above the “baseline” of that profile. The baseline of a given profile is defined to be the line connecting the first and last valid rangels of the profile. This concept is illustrated in Figure 5, where one laser profile from a pyramid structure is depicted. In order for the baseline method to be a valid measurement of surface height, flat surfaces must exist on either side of the scanned object and must be within reach of the laser line. These flat surfaces can be recognized at the beginning and end of a profile in order to create a baseline for the profile.

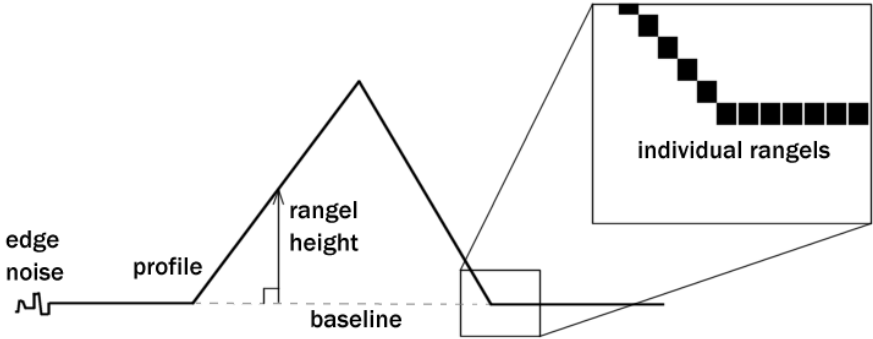


Figure 5. Diagram of profile composition and rangel height computation.

By assuming that the laser profiling system remains stationary, it is reasonable to assume that a significant change in the position of an object being profiled will cause a detectable change in the acquired surface sample geometry of the object, while profiling a motionless object will result in a high degree of similarity between sequential surface samples. Thus, motion of a scanned object can be detected and measured by comparing two or more surfaces. A method is needed for determining the best transformation from one surface to another such that the two surfaces are aligned in space. A transformation from one surface to another can be defined by six parameters, specifically three translations and three rotations. The ICP algorithm<sup>3</sup>, a method for registering a set of points to a reference set, is well suited for the purpose of calculating these parameters.

### 2.2.2 Calibration of the laser profiling system

Both of the cameras used in the laser profiling system are calibrated via the following process. The calibration process is a method whereby perceived positions of points on a known surface are compared to their actual positions, and discrepancies between each pair of values are stored in a table. The table values are used to map future perceived points to their true location in a standard reference frame. Three one-dimensional mappings are performed on a particular surface point to obtain a three-dimensional correction vector for the point. The correction in each dimension is based on a set of geometric curves that characterizes the relationship between perceived position and actual position in that dimension. By using table values based on single points to accurately scale a relationship curve, all perceived point positions in a particular dimension that fall within the domain of the curve can be mapped to points that represent their true values. The directions of the axes referenced by the names  $x$ ,  $y$ , and  $z$  are illustrated in Figure 6.

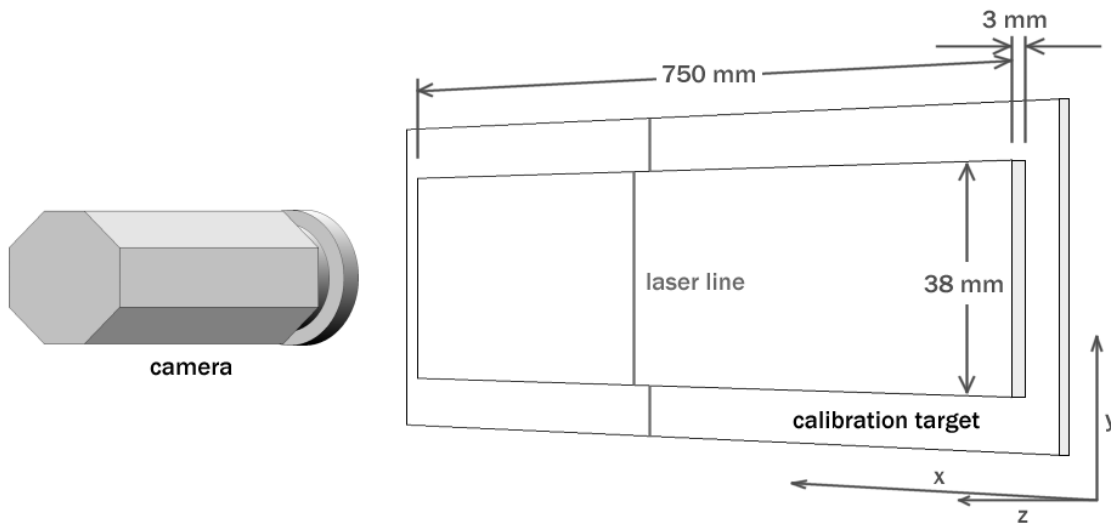


Figure 6. Depiction of laser profiling calibration surface.

A flat surface is used to calibrate the laser profiling system in the  $z$ -dimension. As shown in Figure 6, the  $z$ -axis is defined to be a line perpendicular to the plane across which the laser line is swept, referred to hereafter as the “standard plane”. The  $z$ -axis is parallel to the line segment connecting the two focal points of the cameras, the midpoint of which lies on the standard plane. The calibration surface is raised 3 mm above the standard plane so that the relative height of the raised surface with respect to the standard plane can be measured. Because the height of the calibration surface above the standard plane is constant, it is easy to compare the perceived height values from the camera to their actual height. The calibration algorithm for the  $z$ -dimension begins by acquiring a single relative height datum for every region in an imaginary  $x$ - $y$  grid spanning the calibration surface. For each  $x$ - $y$  point, the perceived height of the surface at the point is recorded. The actual height of the surface is divided by the perceived height, and the resulting correction factor for the current  $x$ - $y$  location is stored in a calibration table. Every time new perceived height data is acquired thereafter, each height datum is multiplied by the correction factor corresponding to its  $x$ - $y$  position to yield a better approximation to its true height. Figure 7 shows surface scans of the calibration surface before and after  $z$ -dimension calibration.

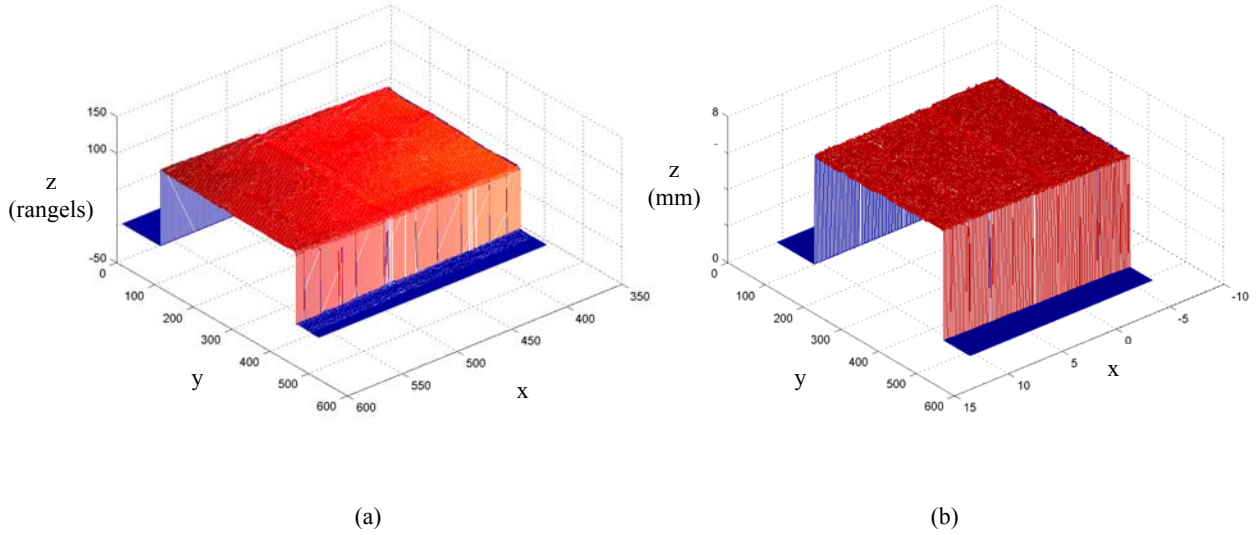


Figure 7. (a) Uncalibrated scan of flat calibration surface, and (b) height-calibrated scan of same surface.

The y-dimension is calibrated using two parallel straight edges 3.8 cm apart. These are the top and bottom edges of the raised surface on the calibration target as illustrated in Figure 6, and they are easily detectable in a laser “profile,” or set of laser range data from a given laser position, as a pair of distinct discontinuities. The edges are parallel to the standard plane and run in the direction of the laser sweep. Because the edges are not parallel to the plane of focus of either camera, the distance between them at any point along the x-axis will not appear constant in the camera images, but instead will appear to decrease as the distance from the plane of focus increases. In order to correct for this distortion, the apparent distance between the edges is stored for each profile. Because the laser line is aligned in the y-direction, every profile can be assigned a single x-coordinate and thus a single y-dimension correction factor. The correction factor is calculated as the true distance between the edges divided by the perceived distance between them. For each data point in a given profile, the distance between the point and the centerline of the two edges is multiplied by the corresponding correction factor for that profile, the number of which is determined by its position along the x-axis, to map the perceived y-coordinate of the point to a more accurate value.

The x-dimension is calibrated according to a derived relationship between the perceived position of a data point along the x-axis and its true position. The parameters used in the derivation are illustrated in Figure 8. The constant parameters  $h_c$  and  $x_c$  denote the height of the camera lens above the standard plane and the horizontal distance from the focal point on the plane, respectively. From the geometry of Figure 8, it can be shown that

$$x_t = \frac{-\left(x_c + \frac{h_c^2}{x_c}\right)x_p}{x_p - \frac{h_c}{x_c}\sqrt{h_c^2 + x_c^2}}, \quad (1)$$

where  $x_t$  is the true position of the data point and  $x_p$  is its perceived position in the camera image. The origin of the x-axis is defined to be the intersection of the optical axis of the camera with the standard plane, or the center of the camera image. Calibration is done by positioning the laser at a known distance from a defined origin (typically 10 mm) and recording the perceived distance in the acquired image (in pixels). The x-dimension correction factor is then calculated by dividing the known distance by the value  $x_t$  of the function at the perceived distance  $x_p$ . This factor multiplies acquired function values at any  $x_p$  to scale them to the appropriate unit.

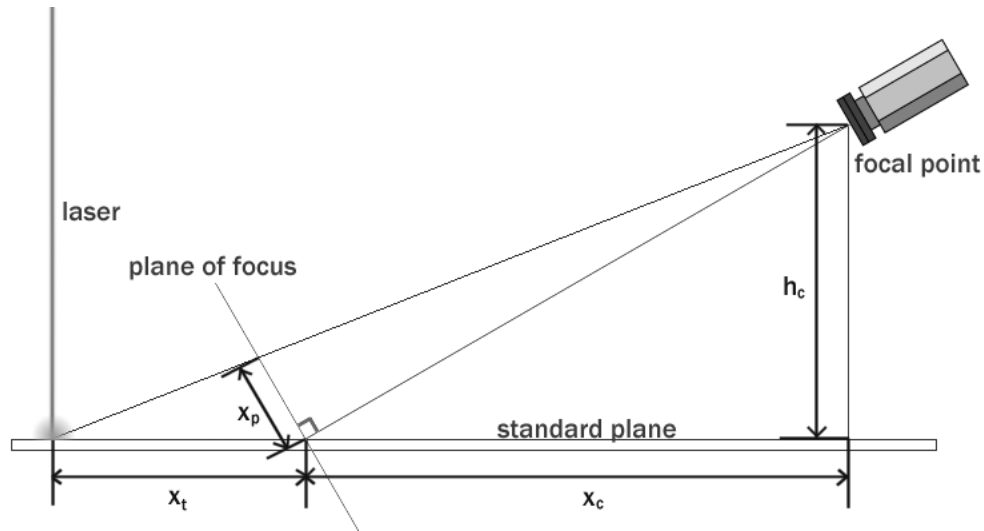


Figure 8. Geometry of camera perception of a point on the standard plane.

### 2.2.3 Surface registration using an ICP algorithm

The basic ICP algorithm<sup>3</sup> operates on two sets of points  $S_1$  and  $S_2$  (not necessarily the same size) and an initial guess of transformation parameters from  $S_1$  to  $S_2$ , and successive iterations of the algorithm work to refine the guess and formulate a better set of parameters to align the two sets in space. The algorithm works by repeatedly matching each point in  $S_2$  with its closest neighbor in  $S_1$  and transforming  $S_2$  so as to minimize a computed sum of the distances between each pair of points. The sum represents the closeness of the two sets, where a smaller sum indicates that the surfaces are more closely aligned and a larger sum indicates a poorer alignment. A stopping criterion for the algorithm is based on this sum such that iterations will continue until the sum is less than some specified limit.

Because a surface sample obtained from laser profiling is simply a set of three-dimensional points, the ICP algorithm can be used to compute transformation parameters from one surface to another. The algorithm will attempt to find a set of translations and rotations such that the two surfaces are as closely aligned as possible. If two such surfaces represent two positions of an object at different points in time (as is the case in the laser profile tracking method), the algorithm will yield an approximation of the object's movement from the first position to the second position. The computational load of the ICP algorithm increases dramatically as the sizes of the two input sets increase, and as a result surface registrations are not computed in real-time for the purpose of animal tracking. Techniques to reduce the number of points needed to represent the surface will be explored.

## 3. EXPERIMENTAL RESULTS

This section presents position measurement results obtained from the reflective marker tracking system and surface measurement results obtained from the laser profile tracking system.

### 3.1 Reflective marker pose tracking results

A photograph of the SPECT instrument under development is shown in Figure 9. The tracking cameras, mirrors, and LED arrays are shown in relation to the gamma cameras. Note the tube with markers visible near the center. The accuracy of the tracking system was tested using three IR reflectors on a plastic phantom. At this point we have tested tracking accuracy in three directions: axially (along the axis of system rotation) and transaxially in  $x$  and  $y$  (horizontal and vertical relative to axis of system rotation). Six target images were used to perform the intrinsic and extrinsic camera calibration. For the three axial measurements and roll angle measurement, the phantom was mounted to  $x$ -,  $y$ -, and  $z$ -translation stages and a rotation stage that were moved via micrometers. Measurements of noise while repeatedly measuring a stationary target have also been made for all six degrees of freedom. The results obtained to date are shown in Tables 1 and 2 below. With a desired accuracy of 0.1 mm over 10 mm of motion, both  $y$  and  $z$  translation measurements are seen to fall within this error range. The  $x$ -axis translation error, at 0.29 mm, is seen to be just above this range. However, it is expected that better calibration using more than six calibration images will reduce this error.

The z-axis rotation (roll) measurement accuracy falls within a desired error range of 0.1 degrees over 10 degrees of rotation. More experiments that measure the two remaining rotations (pitch and yaw) are desirable and planned.

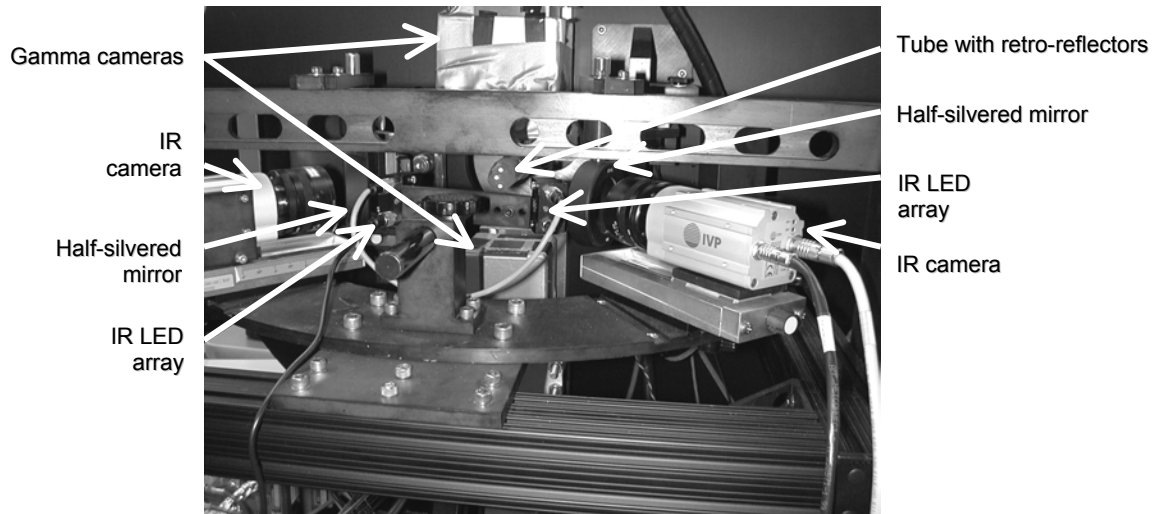


Figure 9. Photograph of SPECT instrument with reflector tracking system components labeled.

Direction	Actual Distance	Result from Tracking System
axial (z)	12.7 mm (micrometer)	12.73 mm
transaxial (x)	12.7 mm (micrometer)	12.41 mm
transaxial (y)	12.7 mm (micrometer)	12.66 mm
Roll (angle about z)	10 degrees	9.98 degrees

Table 1. Reflective marker tracking system measurement results

Direction	Stationary Noise (standard deviation)
axial (z)	0.0013 mm
transaxial (x)	0.0016 mm
transaxial (y)	0.0026 mm
Roll (angle about z)	0.0339 degrees
Pitch (angle about x)	0.0220 degrees
Yaw (angle about y)	0.0281 degrees

Table 2. Tracking noise in all directions with stationary object.

### 3.2 Laser profiling results

A photograph of the laser profile tracking system under development is shown in Figure 10. The lasers and oscillating mirrors are shown in relation to a plastic tube positioned at the typical location of a laser-profiled subject. Both tracking systems use IVP Ranger SAH5 cameras for imaging. The laser profile tracking system also uses the built-in functionality of the cameras to transform laser image frames into individual profiles. The profiling system currently achieves approximate resolutions of 10 rangels/mm in the y and z dimensions and 10 profiles/mm in the x-dimension. A program has been written to calibrate the tracking system, acquire a set of profiles, and compile the profiles to form a 3-D surface. The resulting surfaces are displayed in MATLAB. Figure 4 in section 2.2.1 shows two uncalibrated surfaces acquired by the system.

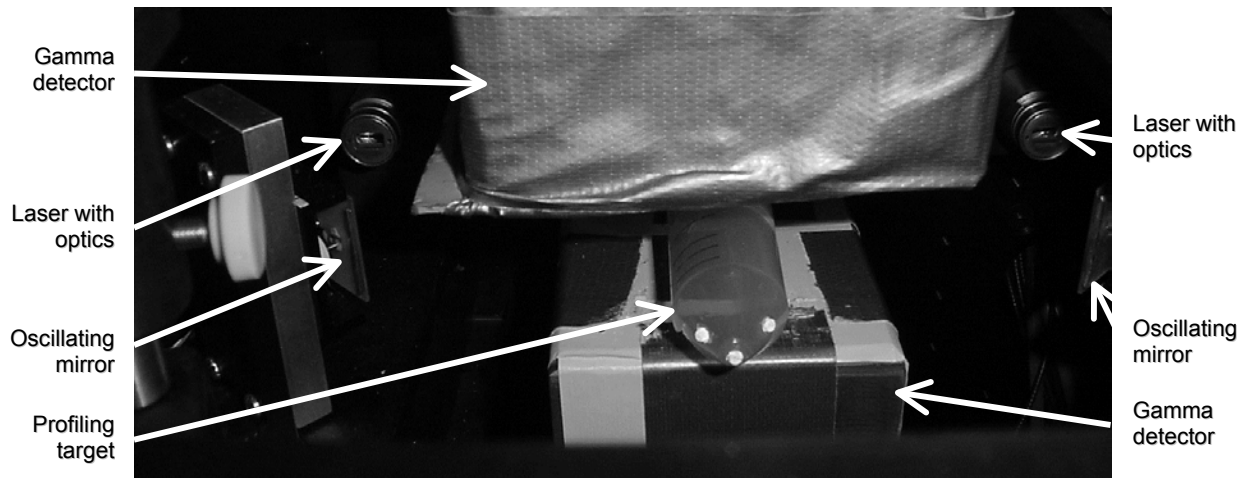


Figure 10. Photograph of SPECT instrument with laser profile tracking system components labeled.

Measurement accuracy of the laser profile system was tested using a pyramid-shaped structure. The system was first calibrated using the technique described above, and a surface was acquired by the system. The actual dimensions of the pyramid and the measurements obtained from the acquired surface are shown in Table 3. A plot of the calibrated pyramid surface is shown in Figure 11. Currently, surfaces are acquired one at a time, where one surface consisting of 200 uniquely positioned profiles is generated in approximately 3 seconds. Such a long acquisition time is not sufficient for the purpose of tracking but is irrelevant to the preliminary task of surface measurement. A possible source of error in the base length measurement is the use of manual laser positioning in the x-dimension calibration process.

Dimension	Actual Value	Profile Result
height (z)	4.8 mm	4.5 mm
base length (x)	22.5 mm	25.0 mm
base width (y)	22.5 mm	22.0 mm

Table 3. Surface measurements from laser profile system.

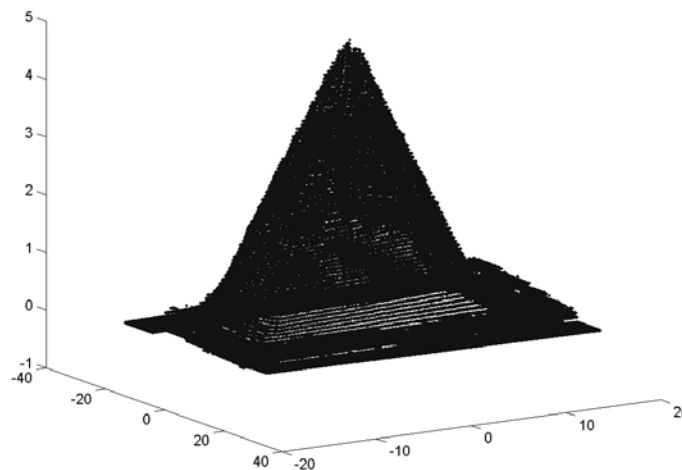


Figure 11. Plot of calibrated pyramid surface used in measurement accuracy test.

The ICP algorithm has been implemented and tested on computer-generated surfaces of 50 to 100 points including paraboloids and planes. The running time of the algorithm on these surfaces was observed to be on the order of 10 seconds per iteration. Typically 5 to 10 iterations were required for satisfactory convergence of the two test surfaces. It is expected that the current ICP algorithm will need to be adapted for this experiment in order to achieve convergence on large laser-generated surfaces.

#### 4. SUMMARY AND FUTURE WORK

Two methods currently under development for small animal tracking have been described, and some preliminary results from each system have been presented. The reflector tracking system has yielded high accuracy measurement results in all three translational degrees of freedom, and work has been done to transform rotation measurements to a standard set of axes in order to simplify future validation experiments on the remaining degrees of freedom. Speed of tracking needs to be improved to meet the desired frame rate of 15 frames/sec. The laser profile tracking system is able to acquire and measure surfaces with reasonably high accuracy by using the calibration technique described in this paper.

The laser profile tracking method has an advantage over the reflector method in that no imaging aids need to be attached to the animal. Future plans for improving the reflector tracking system include the segmentation of natural features from the animal in real time in order to dispense with artificial markers. Future work on the laser profiling system will include increasing the speed of surface acquisition and the ICP algorithm as well as increasing the accuracy of surface measurements.

#### REFERENCES

1. A.G. Weisenberger, B. Kross, S. Majewski, V. Popov, M.F. Smith, B. Welch, R. Wojcik, M. J. Paulus, J. S. Goddard, S. S. Gleason, S.R. Meikle, M. Pomper, "Development of a Restraint Free Small Animal SPECT Imaging System," Academy of Molecular Imaging Annual Conference, San Diego, CA, October 2002.
2. J. Goddard, S. Gleason, R. Kerekes, M. Paulus, A. Weisenberger, M. Smith, B. Welch, and R. Wojcik, "Real-time landmark-based unrestrained animal tracking system for motion-corrected PET/SPECT imaging," Proc. IEEE Medical Imaging Conference, November 2002.
3. P. Besl and N. McKay, "A Method for Registration of 3-D Shapes", *IEEE Trans. Pattern Analysis and Machine Intelligence*, **14**, 239–256, 1992.
4. R. Hartley and A. Zisserman, "Multiple View Geometry in Computer Vision," Cambridge: Cambridge University Press, 2000.
5. B. Horn, "Closed-form solution of absolute orientation using unit quaternions," *Journal of the Optical Society of America*, **4**, 629-642, 1987.